Combined Analytical and Numerical Approach to Study Coil Arrays for Contactless Charging of Batteries in Active Transponders

F. A. Hrebenciuc

Department of Electrical Engineering and Computer Science, Stefan cel Mare University of Suceava,
720229, Romania, phone: +40722385823, e-mail: florin.hrebenciuc@usv.ro

D. Moga, D. Petreus, Z. Barabas, R. Moga

Technical University of Cluj-Napoca,
400114, Romania, phone: +40726362327, e-mails: daniel.moga@aut.utcluj.ro, dorin.petreus@ael.utcluj.ro,
albert.barabas@abbott.com, rozica.moga@math.utcluj.ro

Introduction

When thinking about *transmitting inform*ation in a contactless way, it is easily observable that the wireless transmission systems revolutionized the world of communication. The topic of *energy transmission in a contactless way* is becoming more and more important as the number of applications that can benefit from it increases every day.

It is generally accepted that contactless electrical energy transmission (CEET) has distinct advantages over the conventional energy transmission systems using wires and connectors. The usage of sliding contact by metal-to-metal and carbon brush connection or trailing cable for power delivery to mobile loads cannot avoid problems like wear, exposed live conductors, loss of good connection, and thermal cycling [1].

The circuits for coupling with sensors in a contactless manner can provide the only acceptable solution for power delivery and information exchange when the sensor system has to perform in special conditions. Examples of such conditions are: a requirement of special mobility (large number of freedom degrees), the impossibility of using wires or cables, electrically insulated sensors, totally encapsulated systems for harsh environments, and in-vivo measurement systems.

One can observe, thinking of many emergent applications that must work in situations like the ones mentioned above, that the problem of devising circuits able to transfer both power and information in a contactless manner is of primary importance for many types of sensor systems. The RFID devices that provide extended functionality in terms of independent sensing and monitoring, high communication range and large memory areas are named next generation of UHF RFID tags or higher class RFID tags, characterized by a continuous operation even when they are not powered by the reader as in pure passive UHF RFID systems[2].

The case of the active transponder (active tag) systems used in logistic applications is a typical one: many times the tag has to operates in environments that ask for total (sealed) encapsulation, and still there must be a way for delivering the power to charge its internal battery or capacitor [3] for assuring sensor operation while it is away from the reader. Since in many cases the tag must be attached to a pallet, this paper examines the possibility of using a CEET method for delivering the power for the charging of the tag battery.

CEET systems are generally implemented based on the principle of magnetic induction. A varying magnetic field is generated with energy provided by a first subsystem in order to produce an ac voltage on the second subsystem. This is illustrated in Fig. 1 [4].
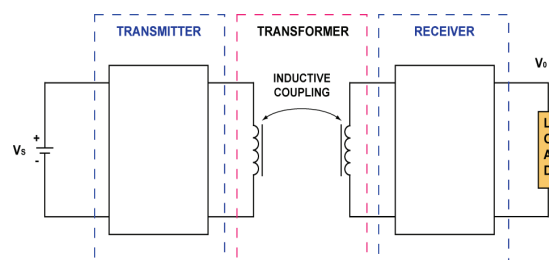

Fig. 1. Block diagram of an inductive CEET

There are two classes of applications: those needing full mobility in which the transformer is an air core one, and those in which sliding or rotation appears, allowing for the usage of a core [5–8].

It is important to observe that due to the specifics of the application the transformer in Fig. 1 is not a "classic" one. The distance between coils could be much larger than usually, it also could be variable from one moment to the other, and there are situations in which the core misses ("air core"). All these considerations led to *the necessity of assessing the efficiency of such transformers based on their geometry and of searching for the best architecture and implementation topologies in terms of power transfer efficiency*. One class of architectures currently proposed is based on resonant operation. Since the operation at resonance must be achieved using the appropriate value of the frequency, this architecture has the advantage of making it possible to adjust the behavior of the system according to changes in the coupling and according to changes of the supply voltage.

Geometry of planar, circularly shaped coils

There are good reasons for focusing on the geometry of planar, circularly shaped coils (Fig. 2). This kind of shape has some advantages. First of all the volume occupied by that type of coils is small. Secondly, it is feasible to produce them with different technologies (even in silicon).
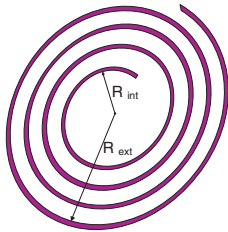

Fig. 2. Circularly shaped coil

Three dimensions characterize these planar, circularly shaped coils: inside radius, outside radius and width. When such devices are intended to be mounted together with the associated hardware, the usual dimensional constraints are: minimum interior radius, maximum exterior radius, and maximum width.
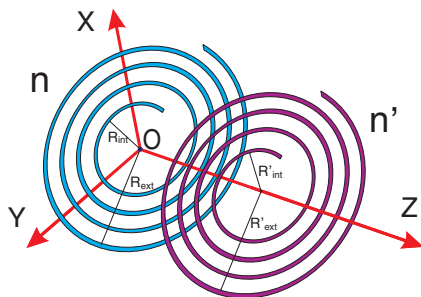

Fig. 3. Two coil setup

These constraints given, one of the goals of the analysis is to provide a characterization of the coil system behavior. That will allow devising a procedure for finding those optimal coil dimensions (which will provide the maximum efficiency).

It is shown that the situation when coils are axially aligned at an established distance can be optimized in a straightforward manner [4], but it is very important to

study the variations of efficiency when perturbations like coil radial misalignment, variation of the axial distance between coils and load variation are present.
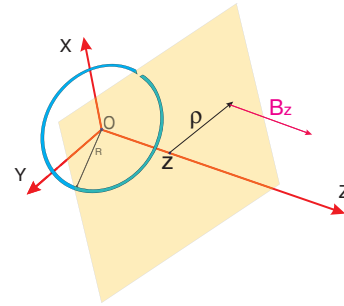

Fig. 4. B_z generated by a turn

For the field generated by the turn with radius R, the Z component of the vector **B** in a point contained in the plane parallel with coil plane, at distance z from it (B_z), and having a distance ρ to the Z axis is represented in Fig. 4.

Analysis of the magnetic field

The analysis and simulation of the magnetic fields generated by coils is currently done with combined analytical and numerical methods or with finite element method [4, 9].

The value of B_z can be computed starting from the Biot-Savart-Laplace formula, an integral formula that enables one to calculate the magnetic field at any space-point due to an electric current. With reference to Fig. 5

$$\mathbf{H} = \frac{1}{4\pi}\int_{(D_c)}\frac{\mathbf{J}\times\mathbf{1_r}}{r^2}\left(A\mathbf{n}\,d\mathbf{l}\right) = $$
$$= \frac{1}{4\pi}\int_{(D_c)}\frac{d\mathbf{l}\times\mathbf{1_r}}{r^2}\left(A\mathbf{nJ}\right) = \frac{i}{4\pi}\oint_{(\Gamma)}\frac{d\mathbf{l}\times\mathbf{1_r}}{r^2}. \quad (1)$$

This further leads to

$$\mathbf{H} = \frac{i}{4\pi}\oint_{(\Gamma)}\frac{d\mathbf{l}\times\mathbf{r}}{r^3}. \quad (2)$$

Considering the circular loop in Fig. 6, and introducing the notations:

$$\overrightarrow{vp} = \{R\cos[t], R\sin[t], 0\}, \quad (3)$$

$$\overrightarrow{vm} = \{x, y, z\}, \quad (4)$$

$$\overrightarrow{vr} = \overrightarrow{vm} - \overrightarrow{vp} = \{x - R\cos[t], y - R\sin[t], z\}, \quad (5)$$

$$\overrightarrow{product} = \partial_t\overrightarrow{vp}\otimes\overrightarrow{vr}, \quad (6)$$

$$num = \left\|\overrightarrow{vr}\right\|^3. \quad (7)$$

It follows that:

$$\overrightarrow{product} = \{Rz\cos[t], Rz\sin[t],$$
$$-Rx\cos[t] + R^2\cos[t]^2 - Ry\sin[t] + R^2\sin[t]^2\}, \quad (8)$$

$$num = \left(z^2 + (x - R\cos[t])^2 + (y - R\sin[t])^2\right)^{3/2}. \qquad (9)$$
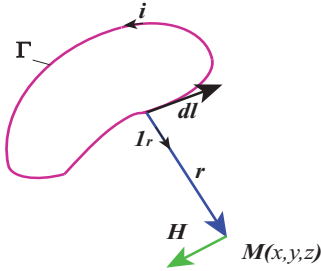

Fig. 5. Computation of the magnetic field intensity produced by a loop of current

Considering only the Z component

$$-Rx\cos[t] + R^2\cos[t]^2 - Ry\sin[t] + R^2\sin[t]^2, \qquad (10)$$

it follows that the ratio that should be integrated is

$$\frac{-Rx\cos[t] + R^2\cos[t]^2 - Ry\sin[t] + R^2\sin[t]^2}{\left(z^2 + (x - R\cos[t])^2 + (y - R\sin[t])^2\right)^{3/2}}. \qquad (11)$$

Introducing $\begin{aligned} x &= \rho\cos[\varphi] \\ y &= \rho\sin[\varphi] \end{aligned}$ this ratio becomes

$$\frac{R^2\cos[t]^2 - R\rho\cos[t]\cos[\varphi] + R^2\sin[t]^2 - R\rho\sin[t]\sin[\varphi]}{\left(z^2 + (-R\cos[t] + \rho\cos[\varphi])^2 + (-R\sin[t] + \rho\sin[\varphi])^2\right)^{3/2}}. \qquad (12)$$
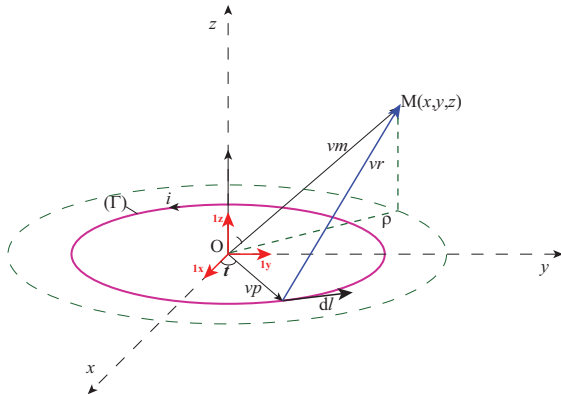

Fig. 6. Determining the magnetic field produced a circular loop of current lying in the x-y plane

Since the generated field has a circular symmetry, the value of φ is not relevant. Considering $\varphi = 0$, the computation of B_z will lead to the following integral, in order to evaluate the field intensity B_z produced in a point lying in the parallel plane at distance z, with an eccentricity ρ, by current I flowing through a circular path of radius R

$$B_z(\rho, R, z) = \frac{\mu_0 I}{4\pi} \int_0^{2\pi} \frac{R(R - \rho\cos t)}{\left(R^2 + z^2 + \rho^2 - 2R\rho\cos t\right)^{3/2}} \, dt, R > 0. \quad (13)$$

This result can be further used in computing the global value due to all n turns of the coil depicted in Fig. 7 ($R_{int} = b_1$, $R_{ext} = b$, $\rho =$ the distance from Z axis)

$$Btotalz(\rho, z, n, b_1, b_2) = \sum_{i=0}^{n-1} B_z\left(\rho, b_1 + \frac{i(b_2 - b_1)}{n-1}, z\right). \quad (14)$$

Numerical approximation for field simulation

Since $z^2 + (R + \rho)^2 > 0$, the integral (3) can be expressed using the elliptic functions as

$$\left(2\left((R^2 - z^2 - \rho^2)\,\text{EllipticE}\left[\frac{4R\rho}{z^2 + (R + \rho)^2}\right] + \right.\right.$$
$$\left.\left. + (z^2 + (R - \rho)^2)\,\text{EllipticK}\left[\frac{4R\rho}{z^2 + (R + \rho)^2}\right]\right)\right) /$$
$$/ \left((z^2 + (R - \rho)^2)\sqrt{z^2 + (R + \rho)^2}\right), \qquad (15)$$

where:

$$\text{EllipticE}(m) = \int_0^{\pi/2} \sqrt{1 - m\sin(\theta)^2} \, d\theta, \qquad (16)$$

$$\text{EllipticK}(m) = \int_0^{\pi/2} \frac{1}{\sqrt{1 - m\sin(\theta)^2}} \, d\theta. \qquad (17)$$
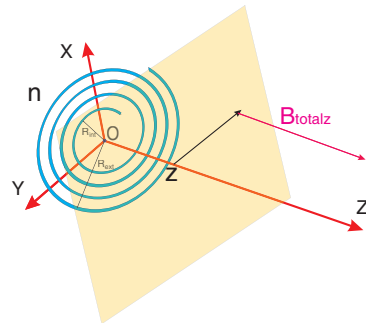

Fig. 7. B_z generated by the whole coil

In order to speed up the computations, two functions based on Pade approximants of the elliptic functions were built in order to approximate EllipticE, and EllipticK over the interval [0,1):

$$fEllipticK = \begin{cases} \dfrac{1.533 - 1.478(0.1 + x) + 0.274(0.1 + x)^2}{1 - 1.193(0.1 + x) + 0.335(0.1 + x)^2 - 0.010(0.1 + x)^3}, if\ x < 0.5 \\[2mm] \dfrac{2.257 - 12.158(-0.8 + x) + 12.723(-0.8 + x)^2}{1 - 6.393(-0.8 + x) + 9.403(-0.8 + x)^2 - 1.435(-0.8 + x)^3}, \end{cases} \quad (18)$$

$$fEllipticE = \begin{cases} \dfrac{1.646 - 1.483(0.2 + x) + 0.292(0.2 + x)^2}{1 - 0.678(0.2 + x) + 0.062(0.2 + x)^2 + 0.002(0.2 + x)^3}, if\ x < 0.5 \\[2mm] \dfrac{1.178 - 5.274(-0.8 + x) + 4.539(-0.8 + x)^2}{1 - 3.903(-0.8 + x) + 2.042(-0.8 + x)^2 + 0.314(-0.8 + x)^3}. \end{cases} \quad (19)$$

For a planar, circularly shaped turn, the numerical simulation produces the variation of $B_z(\rho, R, z)$ represented in Fig. 8, considering an 1 Amp current.
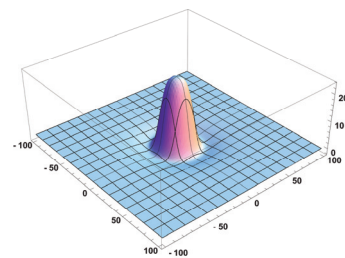

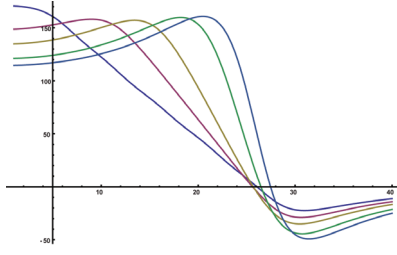**Fig. 8.** $B_z(\rho, 17, 10)$ generated by one turn according to equation (3)

Fig. 9. Variation of $B_z(\rho,5,5,b_1,27)$ for ρ between 1mm and 40mm presents the shapes above for the following values of b_1 (in mm): 7(blue), 13(red), 17(yellow), 22(green), 25(light blue)

Flux based optimization of the power transfer

Three major issues in designing the contactless charger are identified in [10]: transformer geometry (which can increase the coupling coefficient under the constraints in size and weight), the converter topology (which can increase the conversion efficiency) and the battery-charging controller which is needed for proper and safe charging of the battery. The rectifier block can also benefit from new topologies and technologies developed for the passive tags [11].

A flux based analysis of the transformer geometry will be performed in what follows in order to provide design solutions for the optimization of the power transfer.

The distribution of magnetic field H and the magnetic induction Bz were analyzed in order to determine an accurate estimation of the magnetic flux in the air, an approach used also in [12].

The flux generated by a turn through a parallel disc of radius R, place at a distance z can be computed as follows

$$F1(x_0,y_0,R,z,n,b_1,b_2) :=$$
$$= \int_0^{2\pi}\int_0^R Btotalz\left(\sqrt{(x_0+r\cos[\theta])^2+(y_0+r\sin[\theta])^2},z,n,b_1,b_2\right)r\,dr\,d\theta. \quad (20)$$
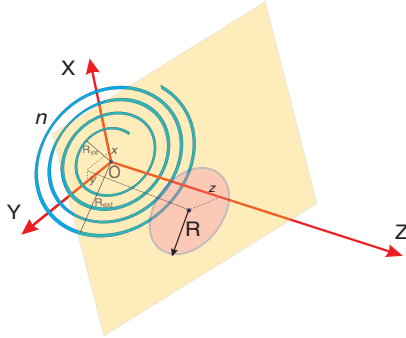

Fig. 10. Parallel disc considered for flux computation

In order to account for the multiple turns of the primary spiral coil, and of the secondary spiral coil a summation formula can be used

$$Ftotal(x_0,y_0,z,m,n,b_1,b_2,B_1,B_2) :=$$
$$= \sum_{i=0}^{m-1} flux2\left[x_0,y_0,B_1+\frac{i(B_2-B_1)}{m-1},z,n,b_1,b_2\right]. \quad (21)$$

The total flux *Ftotal* permits to find the dimensions of primary coil that, when the distance between coils and the

dimensions of secondary coil (that is powering the active tag) are given, will conduct to a maximal value of the flux generated by the primary coil into the secondary coil when the those two coils are coaxial [4].

The situations of interest for the current work are those in which this coaxial alignment constrains is no longer valid. The value of the flux $F1(a,a,R,10,5,17,27))$ produced by a primary coil with 5 turns, having $R_{int}=17$ and $R_{ext}=27$, through a secondary turn of radius R placed at 10mm depends not only on the radius, but also on the eccentricity (a,a) between the center of the coil and the center of the secondary turn (Fig. 11).
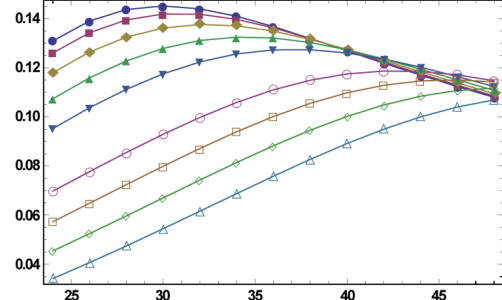

Fig. 11. The curves obtained for the flux $F1(a,a,R,10,5,17,27))$ when R goes between 24 and 48 are represented for each a $\in \{0,3,5,7,9,11,13,15,17\}$

When the mean and the variance of the flux value are represented for each value of the radius the results of Fig. 12 are obtained. The locus of the points (Mean, Variance) for the flux $F1(a,a,R,10,5,17,27))$ when R goes between 24 and 48 represented in Fig. 13 gives an indication the values of R that optimize the transfer of power when no alignement conditiotions are present.
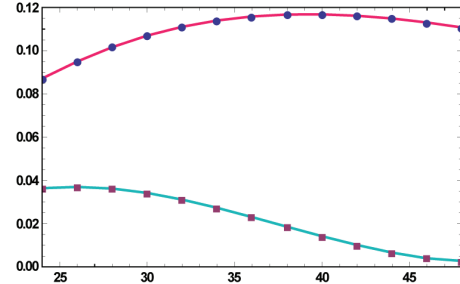

Fig. 12. Mean value of the flux $F1(a,a,R,10,5,17,27))$ when R goes between 24 and 48 represented in red and flux variance in green
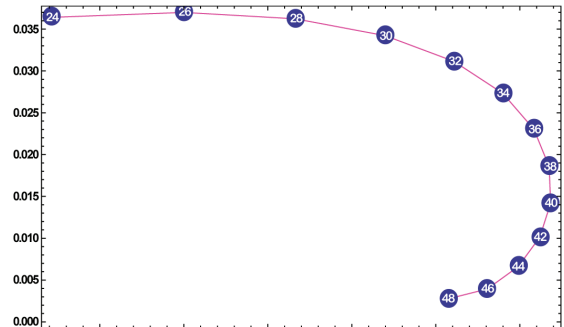

Fig. 13.. Locus of the points (Mean, Variance) for the flux $F1(a,a,R,10,5,17,27))$ when R goes between 24 and 48

Array structures for contactless battery charging

An array (or matrix) charging setup with multiple primary/secondary side devices might be the only solution able to maintain sufficient total equivalent coupling regardless of the position and alignment of the receiving circuit. Both inductive [9] and capacitive [13] solutions are proposed in the literature.

The possibilities of using the planar, circularly shaped geometries analyzed in the previous sections in an array setup are investigated as a CEET method for delivering the power for the charging of the tag battery attached to a pallet (Fig. 14).
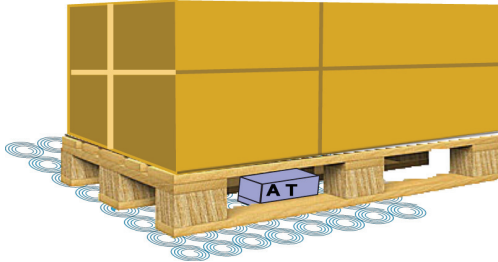

Fig. 14. The placement of a pallet over a coil array to assure powering of the active tag AT attached to the pallet

A setup with four primary coils and a one turn secondary coil sliding in a parallel plane (see Fig. 15) was analyzed.
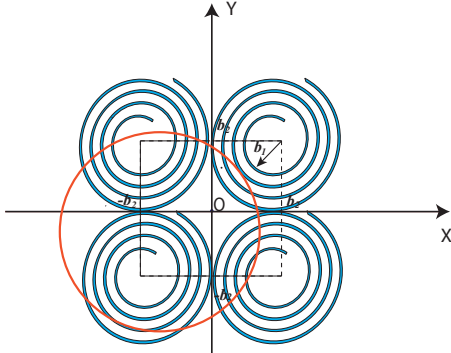

Fig. 15. A setup with four primary coils and a one turn secondary coil sliding in a parallel plane

The value of B_z can be computed for this setup using equation (4) for each of the four coils

$$Btotal4(x,y,z,n,b_1,b_2) :=$$

$$= Btotalz\left(\sqrt{(x-b_2)^2 + (y-b_2)^2}, z, n, b_1, b_2\right) +$$

$$+ Btotalz\left(\sqrt{(x+b_2)^2 + (y-b_2)^2}, z, n, b_1, b_2\right) +$$

$$+ Btotalz\left(\sqrt{(x-b_2)^2 + (y+b_2)^2}, z, n, b_1, b_2\right) +$$

$$+ Btotalz\left(\sqrt{(x+b_2)^2 + (y+b_2)^2}, z, n, b_1, b_2\right). \quad (22)$$

The variation of Btotal4 over an square of 200mm x200mm is represented in Fig. 16 and Fig 17. The superposition of negative values of B_z is producing the negative peak indicated in Fig. 17. The superposition of positive and negative values of B_z may lead to the cancelling of their effect: if the radius of the receiving turn is too small there will be positions where the total flux is zero (see Fig. 18). Since the placement of the pallet over the coil array is random, a canceling situation like this may lead to an impossibility to transfer power toward the active tag. A larger radius of the receiving coil may not only avoid this (see Fig. 19) but also optimize the transfer in accordance to the results of Fig. 13.
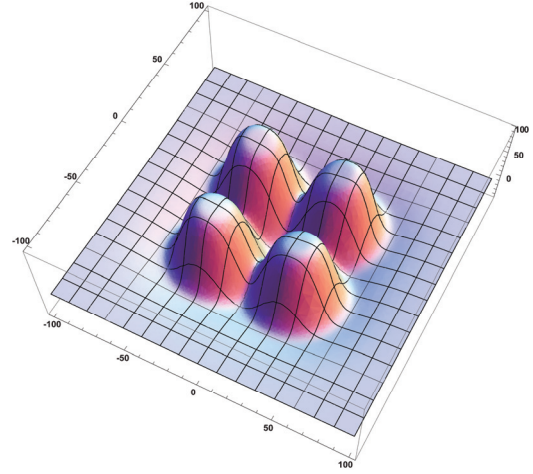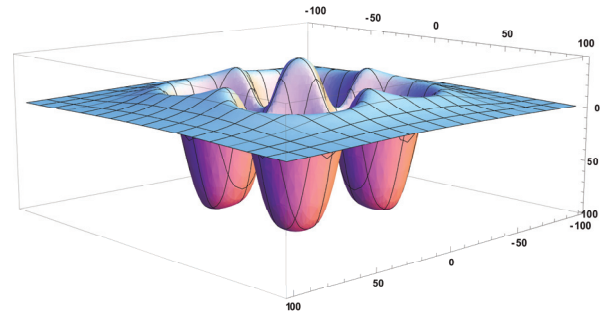

Fig. 16. *Btotal4*[x,y,10,5,17,27]

Fig. 17. Flipped surface showing the superposition of negative values around the centre of the four coil system
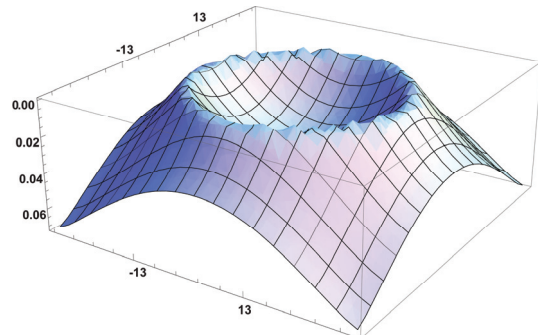

Fig. 18. The absolute value of the flux generated by *Btotal4* through a disc of radius 32mm placed at an axial offset (x,y) at z=10mm
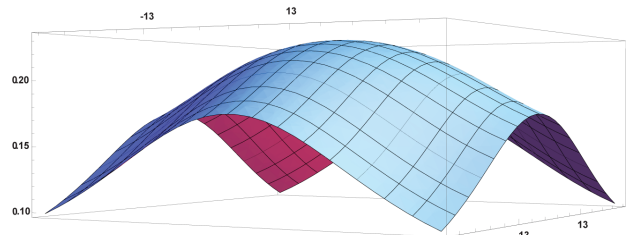

Fig. 19. The flux generated by *Btotal4* through a disc of radius 45mm placed at an axial offset (x,y) at z=10mm

41

Conclusions

A realistic model for the computation of the magnetic field intensity generated by the transmitter coil was developed. In this model the planar spiral coils were considered as being a collection of n circular turns with radius ranging from R_{int} to R_{ext}, coaxially placed in the XOY plane of an XY Z coordinate system. This model was implemented in Mathematica. Numerical values, 2D and 3D graphical representations of the field intensity and of the flux were generated with this application in order to analyze the issues associated with the misalignment of the primary and secondary coil. An array setup is proposed for dealing with the situation of random placement associated with the usage of the active transponder attached to a pallet.

References

1. **Klontz K. W., Divan D. M., Novotny D. W., Lorenz R. D.** Contactless power delivery system for mining applications // IEEE Transactions on Industry Applications, 1995. – Vol. 31(1). – P. 27–35.
2. **Janek A., Steger C., Preishuber–Pfluegl J., Pistauer, M.** Lifetime Extension of Higher Class UHF RFID Tags using special Power Management Techniques and Energy Harvest–ing Devices // Power–aware Computing Systems, Dagstuhl Seminar Proceedings 0704, 2007.
3. **Yeager D. J., Powledge P. S., Prasad R., Wetherall D., Smith J. R.** Wirelessly–charged UHF tags for sensor data collection // IEEE International Conference on RFID. – Las Vegas, Nevada, USA), 2008. – P. 320–327. DOI: 10.1109/RFID.2008.4519381.
4. **Moga D., Dobra P.** Smart Sensor Systems. – Mediamira Science Publisher, 2006. – 141 p.
5. **Barnard J. M., Ferreira J. A., van Wyk J. D.** Optimising sliding trans–formers for contactless power transmission systems // 26th Annual IEEE Power Electronics Specialists Conference (PESC '95), 1995. – Vol. 1. – P. 245–251. DOI: 10.1109/PESC.1995.474819.
6. **Ryu Myunghyo, Park Yonghwan, Baek Juwon, Cha Honnyong**. Comparison and analysis of the contactless power transfer systems using the parameters of the contactless transformer // 37th IEEE Power Electronics Specialists Conference (PESC '06), 2006. – P. 1–6. DOI: 10.1109/PESC.2006.1712216.
7. **Papastergiou K. D., Macpherson D. E.** An airborne radar power supply with contactless transfer of energy part i: Rotating transformer // IEEE Transactions on Industrial Electronics, 2007 – Vol. 54(5). – P. 2874–2884. DOI: 10.1109/TIE.2007.902044.
8. **Kim Yoon–Ho, Jin Kang–Hwan**. Design and implementation of a rectangular–type contactless transformer. // IEEE Transactions on Industrial Electronics, 2011. – Vol. 58(12). –P. 5380–5384. DOI: 10.1109/TIE.2011.2130490.
9. **Achterberg J., Lomonova E. A., de Boeij J.** Coil array structures compared for contactless battery charging platform // IEEE Transactions On Magnetics, 2008. – No. 5(44). – P. 617–622. DOI: 10.1109/TMAG.2008.917022.
10. **Kim Chang–Gyun, Seo Dong–Hyun, Ypu Jung–Sik, Park Jong–Hu, Cho Bo H.** Design of a contactless battery charger for cellular phone // IEEE Transactions on Industrial Electronics, 2001. – No. 6(48). – P. 1238–1247.
11. **Liu Dong–Sheng, Li Feng–Bo, Zou Xue–Cheng, Liu Yao, Hui Xue–Mei, Tao Xiong–Fei.** New analysis and design of a RF rectifier for RFID and implantable devices // Sensors, 2011. – No. 11. – P. 6494–6508. DOI: 10.3390/s110706494.
12. **Lastowiecki J., Staszewski P.** Sliding transformer with long magnetic circuit for contactless electrical energy delivery to mobile receivers \\ IEEE Transactions on Industrial Electronics, 2006. – Vol. 53(6). – P. 1943–1948. DOI: 10.1109/TIE.2006.885473.
13. **Liu Chao, Hu Patrick Aiguo, Wang Bob, Nair Nirmal–Kumar C.** A capacitively coupled contactless matrix charging platform with soft switched transformer control // IEEE Transactions on Industrial Electronics, 2011 – Vol. PP. – Iss. 99. – P. 1–11. DOI: 10.1109/TIE.2011.2172174.

F. A. Hrebenciuc, D. Moga, D. Petreus, Z. Barabas, R. Moga. Combined Analytical and Numerical Approach to Study Coil Arrays for Contactless Charging of Batteries in Active Transponders // Electronics and Electrical Engineering. – Kaunas: Technologija, 2012. – No. 7(123). – P. 37–42.

This paper introduces a combined analytical and numerical approach in order to study the suitability of a coil array for contactless transfer of the energy needed for the charging of batteries in active transponders. The way in which the geometry of the coil system influences the efficiency of the transfer is analyzed based on flux computation. An array of planar, circularly shaped primary coils is proposed as a solution to transmit the energy to a secondary coil, contained in the active tag, for situations of random placement of the active tag above the coil array. Ill. 19, bibl. 13 (in English; abstracts in English and Lithuanian).

F. A. Hrebenciuc, D. Moga, D. Petreus, Z. Barabas, R. Moga. Kombinuotas analitinis ir skaitmeninis ričių masyvų bekontakčiam baterijų krovimui aktyviuose transponderiuose tyrimo metodas // Elektronika ir elektrotechnika. – Kaunas: Technologija, 2012. – Nr. 7(123). – P. 37–42.

Pristatomas kombinuotas analitinis ir skaitmeninis metodas, skirtas ričių masyvų tinkamumui bekontakčiam baterijų krovimui aktyviuosiuose transponderiuose tirti. Analizuojama, kaip ričių sistema veikia energijos perdavimo efektyvumą, skaičiuojant sroves. Planarinių apskritimo formos pirminių ričių masyvas pasiūlytas kaip energijos perdavimo į antrinę ritę, esančią priėmimo pusėje, sprendimas, atsižvelgiant į atsitiktinę ričių tarpusavio padėtį. Il. 19, bibl. 13 (anglų kalba; santraukos anglų ir lietuvių k.).